International Journal of Engineering, Mathematical and Physical Sciences
ISSN: 2517-9934
Vol:10, No:12, 2016

Loading Factor Performance of a Centrifugal Compressor Impeller: Specific Features and Way of Modeling

K. Soldatova, Y. Galerkin

Abstract**—**A loading factor performance is necessary for the modeling of centrifugal compressor gas dynamic performance curve. Measured loading factors are linear function of a flow coefficient at an impeller exit. The performance does not depend on the compressibility criterion. To simulate loading factor performances, the authors present two parameters: a loading factor at zero flow rate and an angle between an ordinate and performance line. The calculated loading factor performances of non-viscous are linear too and close to experimental performances. Loading factor performances of several dozens of impellers with different blade exit angles, blade thickness and number, ratio of blade exit/inlet height, and two different type of blade mean line configuration. There are some trends of influence, which are evident – comparatively small blade thickness influence, and influence of geometry parameters is more for impellers with bigger blade exit angles, etc. Approximating equations for both parameters are suggested. The next phase of work will be simulating of experimental performances with the suggested approximation equations as a base.

Keywords**—**Centrifugal compressor stage, centrifugal compressor, loading factor, gas dynamic performance curve.

NOMENCLATURE

b	width of channel
c_u	tangential component of absolute flow velocity
c_p	specific heat at constant pressure
D	diameter
h_{fr}	disc friction head
h_{lk}	loss of a head due to seal leakage
h_T	theoretical head
H_i	head transmitted
K_{pd}	empirical coefficient of velocity diagram
K_μ	empirical coefficient of viscosity influence
$\frac{l}{t}$	cascade solidity
$\bar{m}$	mass flow rate
M_u	blade Mach number
N_i	the internal power, i.e. all power transferred to gas
N_{fr}	the power of outer discs' surfaces friction
N_{lk}	the power a gas portion that leaks through the labyrinth seal
N_T	the so-called theoretical power that is transferred by impeller blades
p	pressure
T	temperature
u	blade velocity
$\bar{V}$	volumetric flow rate
w	relative velocity
z	number of blades
Φ	flow rate coefficient
β_{bl}	blade angle
$\beta_{fr\,sc}$	non-dimensional coefficient of disk friction
β_{lk}	non-dimensional leakage coefficient
β_T	angle of a loading factor performance inclination
δ	blade thickness
φ	flow coefficient
μ'	turbulent dynamic viscosity
π	3.14
ρ	density
τ	shear stress, blade blockade factor
ψ_T	loading factor

A. Subscripts

0	impeller inlet
1	impeller blade row inlet
2	impeller exit
imp	impeller
inl	inlet
des	design
max	maximum

B. Abbreviation

CFD Computational Fluid Dynamics

I. INTRODUCTION

TECHNICAL power that is supplied to gas by an impeller is divided into three components:

$$N_i = N_T + N_{fr} + N_{lk}. \quad (1)$$

Power N_{fr} and N_{lk} are converted into heat. Their origin is illustrated in Fig. 1.

Equation (1) is transformed into the equation of heads by division on a stage flow rate:

Kristina Valerievna Soldatova is with Peter the Great St. Petersburg Polytechnic University, Russian Federaton (phone: +7-905-220-50-70 fax: 8-812-552-98-29; e-mail: buck02@list.ru).

Yuri Borisovich Galerkin is with Peter the Great St. Petersburg Polytechnic University, Russian Federaton (phone: +7-921-942-73-40; fax: 8-812-552-98-29; e-mail: yury_galerkin@mail.ru).

$$h_i = h_T + h_{fr} + h_{lk}, \quad (2)$$

Heads h_{fr} and h_{lk} are presented in non-dimensional mode as rates of theoretic head. Coefficients of disk friction and leakage are presented in (3):

$$h_i = h_T\left(1 + \beta_{fr} + \beta_{lk}\right) \quad (3)$$

Leakage coefficient is a ratio of the mass flow through the labyrinth seal of a shroud to the mass flow through the stage.

The coefficient of disk friction is determined by shear stress on its outer surface. Shear stress depends on the turbulent flow dynamic viscosity μ' and circumferential velocity gradient as it is shown in Fig. 1. That is:

$$\tau_{mò} = \mu' \frac{\partial c_u}{\partial b} \sim \mu' \frac{u}{B}.$$

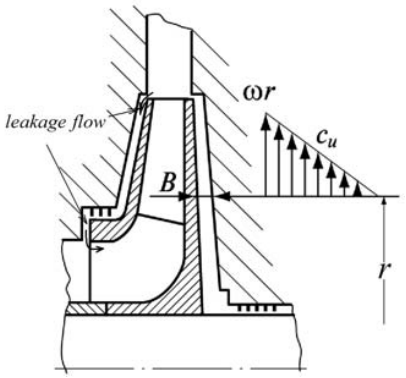

Fig. 1 Leakage flow and shear stress friction due to velocity gradient in an impeller – body gap

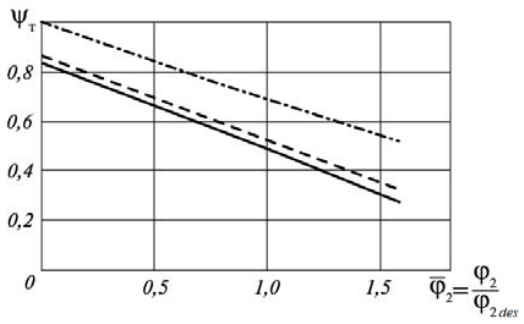

Fig. 2 Loading factor performance of an impeller with Φ_{des} = 0.048, $\psi_{T\,des}$ = 0.47. solid – measured, dash – inviscid, dot-dash - an infinite number of blades

There are effective ways to estimate these coefficients. One-dimensional method is presented in [1]. CFD calculations are presented in [2]. The values of the coefficients for mean specific speed stages are 0.03-0.05. We can assume that the calculation of the coefficients of friction and the leakage disk has satisfactory engineering solution. Therefore, the analysis of a head performance must be concentrated on its main part – loading factor performance.

Fig. 2 from [3] shows the typical measured loading factor performances, the same performance calculated as for inviscid flow and performance of the ideal impeller with infinite blade number. Inviscid calculations are fast and cheap. The results are close to the performances of real impellers. The aim of the work is systematic study of impellers with different geometry parameters and elaboration of approximation equations for numerical study results. The simulation of real impellers' performances on the base of this work is the next step.

II. Basic Features of a Theoretical Head Performance

The value of theoretical head is determined by the "basic equation of turbomachinery" – after Leonhard Euler:

$$h_T = c_{u2} u_2. \quad (4)$$

Equation (4) is valid if a flow has no tangential velocity at an entrance, c_{u1} = 0. This is typical of the centrifugal compressor impellers.

Square of a blade speed as a denominator in (4) performs it to the equation of a loading factor:

$$\psi_T = c_{u2} / u_2 \quad (5)$$

Formally, the problem of a loading factor calculation is easily solved. From the triangle of velocities at the exit of the impeller should be:

$$\psi_T = 1 - \varphi_2 ctg\,\beta_2, \text{ where } \beta_2 = \beta_{bl2} - \Delta\beta. \quad (6)$$

For axial compressor impeller, this equation is used. A lag angle $\Delta\beta$ at an impeller exit is comparatively small and only slightly dependent on flow coefficient. The kinematics of flow in a centrifugal impeller is more complicated. This leads to numerous semi-empirical formulae applied to design flow rate only. These formulae analysis is not an aim of the work. However, the aim of the work is to study principle of a loading factor performance in a whole.

In [4] are presented numerous head performances of gas industry centrifugal compressors. One example is shown in Fig. 3.

Calculated performance in a process of design was made by the 5th version of the Universal modeling method [5]. The head transmitted to gas is measured by the temperature rise: $H_i = c_p \cdot \Delta T_i = 2010 \cdot \Delta T_i$ (air). The performance is almost linear, as in all other known cases. The trend of deviation from linearity manifests itself at high flow rates. This is the effect of gas compressibility. The continuity equation establishes a relationship between the flow rate at the exit of an impeller and the flow rate of the compressor:

$$\bar{V}_{inl} = \frac{\bar{m}}{\rho_{inl}} = \frac{\rho_2}{\rho_{inl}} \pi D_2 b_2 \varphi_2 u_2 . \quad (7)$$

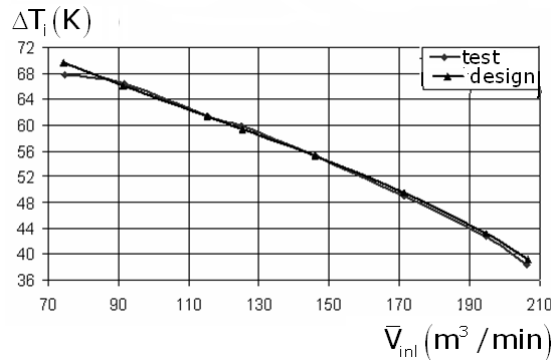

Fig. 3 Gas total temperature rise in a pipeline compressor. Air plant test and design calculation

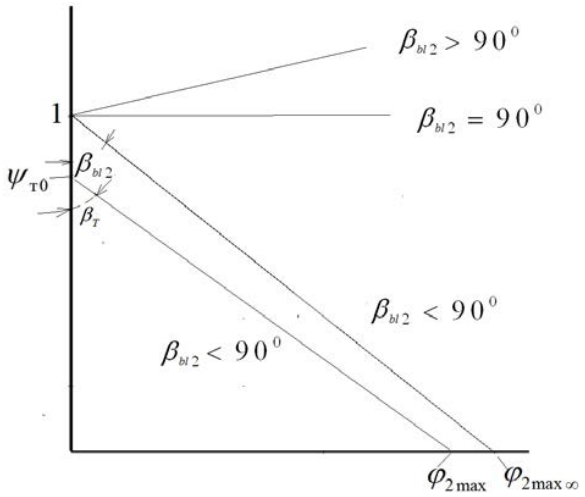

Fig. 4 Loading factor performances of ideal impellers with infinite number of blades and a real impeller performance with $\beta_{bl2} < 90^0$

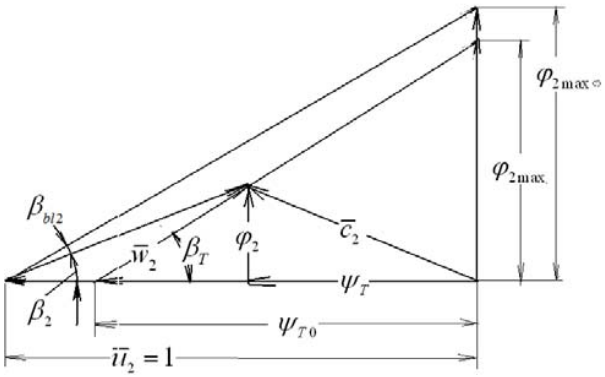

Fig. 5 Exit velocity triangle. A loading factor performance is linear

The coefficient φ_2 determines the value of a loading factor according to (6). At high flow rate gas density ρ_2 decreases rapidly. It leads to non-linear character of a performance. In [6], it is shown that performances in coordinates $\psi_T = f(\varphi_2)$ of tested model stages are linear and do not depend on compressibility.

Fig. 4 shows the load factor performances of ideal impellers with an infinite number of blades. They are linear as flow angle is equal to a blade exit angle, i.e. the angle of imaginative flow is constant. The performance of a real impeller with a blade exit angle < 90^0 is shown there too. The performance is linear inside of a real impeller flow rate range and is extrapolated beyond its limits.

From (6) it follows that if the angle $\beta_{bl2} < 90^0$, the ideal impeller does not create circumferential velocity of flow at a maximum flow coefficient $\varphi_{2\max\infty} = tg\beta_{bl2}$. A loading factor is zero. At zero flow rate the loading factor is $\psi_{T0\infty} = 1$ at any blade exit angle. The angle of a performance inclination is equal to the exit blade angle $\beta_{T\infty} = \beta_{bl2}$.

There is no evidence that outside of a real impeller flow rate range the performance is linear. However, the linear extrapolation points on values of the two factors that determine a loading factor performance. There are:

- $\psi_{T0} < 1$ - a loading factor at zero flow rate,
- $\beta_T \leq \geq \beta_{bl2}$ - an angle of a performance inclination.

Fig. 5 shows the velocity triangle at an impeller exit. A loading factor performance is linear.

The line inclined at the angle of the line β_T it at the same time the loading factor performance shown in Fig. 4. The function $\psi_T = f(\varphi_2)$ is simple.

The program method of universal modeling [3]:

$$\psi_T = \psi_{T0} - \varphi_2 ctg\beta_T . \quad (8)$$

To calculate a loading factor at design flow rate, there are two semi-empirical equations [7]:

$$\psi_{T\,des} = 1 - \varphi_2 \cdot ctg\beta_2 = 1 - \varphi_2 \cdot ctg\beta_{bl2} - \Delta\bar{c}_{u2\,des}, \quad (9)$$

$$\Delta\bar{c}_{u2\,des} = 1 - K_\mu \frac{\psi_{T\,des}}{2z_{bl2}(l_{bl}/D_2)K_{pd}} . \quad (10)$$

There are some equations for ψ_{T0} also. The authors hope to develop a less arbitrary way of the performance modeling.

From (6) and (9), the equation for a lag angle as function of flow coefficient is defined as:

$$\beta_2 = arctg\left(\frac{1}{\frac{1-\psi_{T0}}{\varphi_2} + ctg\beta_T}\right) \quad (11)$$

The angle of the flow varies from zero at a φ_2 = 0 to its minimal value at a maximum flow coefficient. The latter is

valid for $\beta_T < 90^0$. Accordingly, a lag angle changes from $\Delta\beta = \beta_{bl2}$ at zero flow to $\Delta\beta = \beta_{bl2} - \beta_2 arctg(\varphi_{2\max})$ at maximum flow rate.

By analogy with the ideal impeller, we assume that the basic geometrical parameter determining a loading factor performance is a blade exit angle β_{bl2}. The number of blades, their thickness, the relative height of the inlet and outlet, the shape of the median line - i.e. load distribution - can also influence the shape parameters and characteristics. These parameters were studied in the numerical experiment.

III. Method of Calculation

Calculation study was carried out by a computer program 3DM.023, which has long been used in the design practice. The program is based on the representation of 3D flow by two two-dimensional flows:

- axially symmetric flow at infinite number of blades;
- flow on several blade to blade axially symmetric surfaces along blade height.

Fig. 6 demonstrates quasi – orthogonal lines for axially symmetric flow calculation.

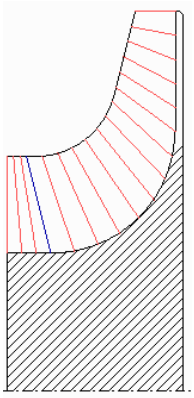

Fig. 6 Quasi – orthogonal lines for axially symmetric flow calculation

Fig. 7 demonstrates a blade cascade on an axially symmetric surface and its conform transformation.

Flow is assumed as expected inviscid and steady. The equations of energy, continuity, equilibrium, perfect gas are solved in iterative process. Flow on blade to blade surfaces is calculated by Zoukovsky vortex theory. Kutta-Zoukovsky postulate is applied as the flow exit condition.

Fig. 8 presents a sample of graphic information in course of calculation in the computer program 3DM.023.

Fig. 9 represents comparison of 3DM.023 velocity diagrams with velocity diagrams defined by measured pressures at the surface of the blades [3].

If a flow coefficient is $\Phi \geq \Phi_{des}$, then the main difference of diagrams takes place near a blade exit. Wake takes place in regions of blades' unload. For large positive incidence angles ($\Phi < \Phi_{des}$), wake low-energy zone occupies a large part of the channel. It caused significant difference of diagrams. Interestingly, this difference does not violate the linear character of a measured loading factor performance.

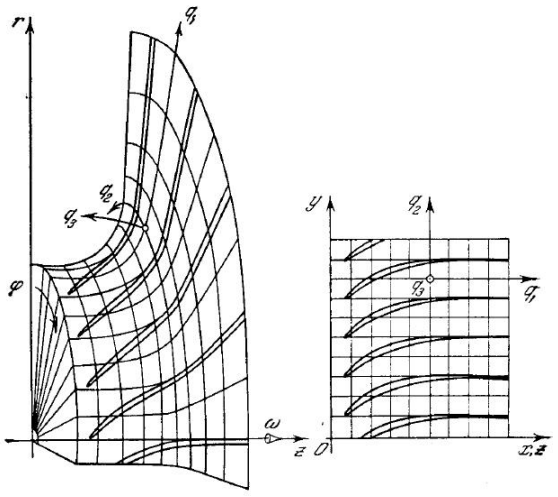

(a) (b)

Fig. 7 Blade cascade on an axially symmetric surface (a), and its conform transformation (b)

IV. Objects of Computational Experiment

In [6], a comparison of measured and calculated by a computer program 3DM-023 loading factor performances is presented. The calculated performances lie higher, but direction of performances is very close. The authors suggest using of the calculation study as a basis for modeling of real loading factor performance as the next stage of their work.

Eight series of studied impellers are based on the impellers of tested model stages. All impellers have the blades of cylindrical shape disposed in a radial part of impellers. Main geometry parameters of the impellers are presented in Table I.

The range of gas dynamic and geometry parameters: Φ_{des} = 0.027-0.075, ψ_{Tdes} = 0.47-0.68, $\bar{D}_1$ = 0.514-0.60, $\bar{b}_1$ = 0.054-0.099, $\bar{b}_2$ = 0.034-0.07, $\bar{D}_h$ = 0.289-0.416, β^0_{bl1} = 20-28, β^0_{bl2} = 30-79, z_{imp} = 11-17.

Information about the shape of the blades in the table:

- "Arcs." - the mean line of the blade is an arc of a circle.
- "l.c." - the mean line is optimized by a load control [3].

Six impellers (##3-8) were also calculated with arc blades. The geometrical parameters of the eight series of impeller variants (all with arc blades) were changed as follows:

- thickness of the blade twice above and twice below a nominal.
- the number of blades reasonably bigger and lower than the nominal.
- the height of the blades at the outlet reasonably bigger and lower than the nominal.

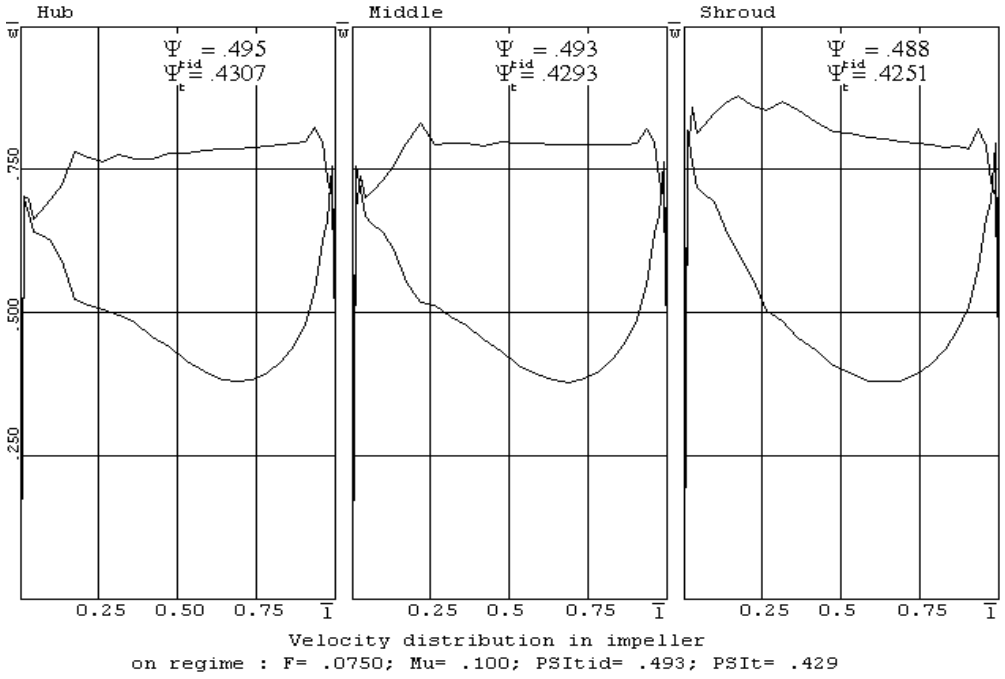

(a)

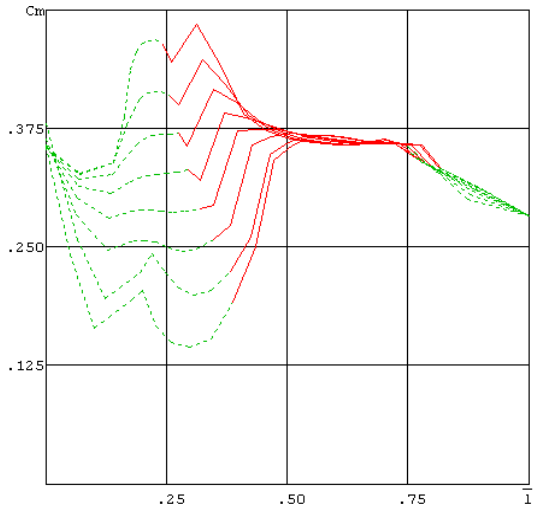

(b)

Fig. 8 Sample of graphic information – the computer program 3DM.023 (a) velocity diagrams: hub, mean, shroud, (b) 0 meridiam velocities at eight blade to blade surfaces

Variants were also calculated with a proportional change in the height of the blades as a whole. This parameter in the calculation of non-viscous flow turned out to be insignificant. To calculate performance parameters β_T and ψ_{T0}, the linear character of a loading factor performance is used:

$$\beta_T = arctg \frac{\varphi'_{2(1)} - \varphi'_{2(1)}}{\psi_{T(2)} - \psi_{T(1)}}. \quad (12)$$

$$\psi_{T0} = \psi_{T(2)} + \varphi'_{2(2)} ctg\beta_T. \quad (13)$$

To calculate the flow rate at an impeller inlet, the continuity equation is applied:

$$\varphi_2 = \frac{\Phi}{4\bar{b}_2\tau_2}\frac{\rho_0^*}{\rho_2}. \quad (14)$$

Here a blade blockade factor is:

$$\tau_2 = 1 - \frac{z \cdot \bar{\delta}}{\pi \cdot \sin \beta_{bl2}} \cdot \qquad (15)$$

It is believed that the trailing edge of the blades are blunt.

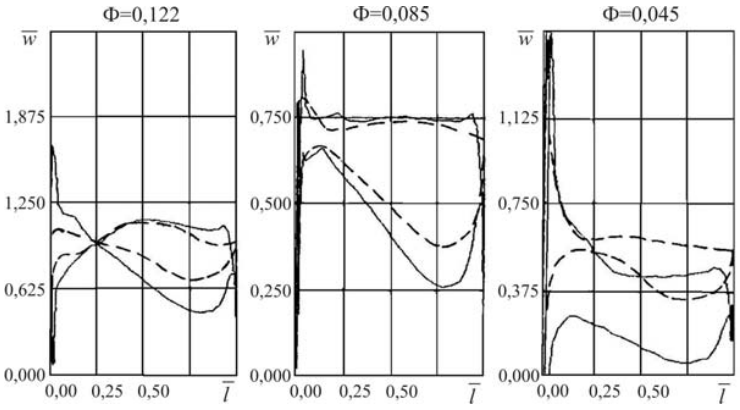

Fig. 9 Comparison of 3DM.023 velocity diagrams with velocity diagrams defined by measured pressures at the surface of the blades. Φ_{des}=0.085. Calculated – solid lines, measured – dashed lines

TABLE I
MAIN GEOMETRY PARAMETERS OF THE STUDIED IMPELLERS

№	1	2	3	4
Name/Parameter	028	038	048	055
$\bar{b}_2$	0.0444	0.0487	0.0576	0.055
$\bar{D}_1$	0.514	0.565	0.534	0.592
$\bar{b}_1$	0.0589	0.0827	0.0884	0.089
$\bar{D}_h$	0.373	0.350	0.289	0.337
β^0_{bl1}	25	25	23	22
β^0_{bl2}	30.3	34	30	47
z_{imp}	15	13	11	13
Mean line shape	arc	arc	l.c.	l.c.
№	5	6	7	8
Name/ Parameter	060	064	K101-1	K101-4
$\bar{b}_2$	0.0606	0.070	0.050	0.034
$\bar{D}_1$	0.570	0.57	0.600	0.534
$\bar{b}_1$	0.0990	0.099	0.0928	0.054
$\bar{D}_h$	0.290	0.290	0.345	0.416
β^0_{bl1}	28	28	27	20
β^0_{bl2}	32	32	79	44
z_{imp}	11	11	17	14
Mean line shape	l.c.	l.c.	l.c.	l.c.

According to [6], compressibility does not affect loading performances of real impeller in coordinates $\psi_T = f(\varphi_2)$. Inviscid flow calculations demonstrate the same. All calculations are executed at $M_u = 0{,}1$. The ratio of densities in (14) is practically equal to 1.

V. The Results of Computational Studies

Fig. 10 presents typical loading factor performances calculated by above method. Fig. 10 demonstrates performances of the eight original impellers (Table I). but all with arc blades. For each impeller the performances were calculated with different blade thickness.

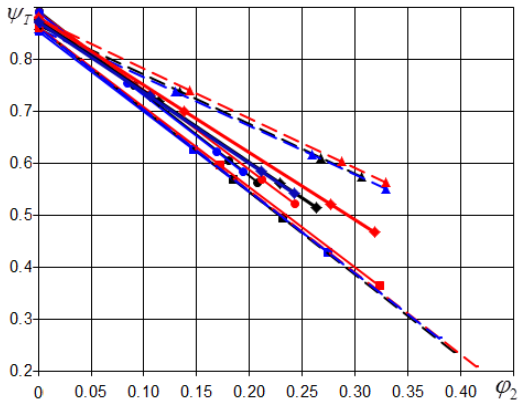

Fig. 10 Loading factor performances of eight impellers with different blade thickness

VI. Influence of the Blade Thickness

The impeller #1 has β_{bl2}= 30.3^0. Its angle β_T= 32.2^0 at $\bar{\delta}_{bl}$= 0.67 – 1.35%. At $\bar{\delta}_{bl}$= 2.7% it is more on 1.1^0. A loading factor ψ_{T0}= 0.893 is independent of the blade thickness.

The impeller #2 has β_{bl2}=34^0. Its angle β_T= 36.2^0 at $\bar{\delta}_{bl}$= 1-2%. At $\bar{\delta}_{bl}$= 4% it is more on 1.3 ^{0}. A loading factor ψ_{T0}= 0.872-0.881 is bigger when the blades are thicker.

The impeller #3 has β_{bl2}=30^0. Its angle β_T= 32.3-33^0 at blade thickness $\bar{\delta}_{bl}$= 0.7-2.8%. A loading factor ψ_{T0}= 0.854-0.862.

The impeller #4 has β_{bl2}=47^0. Its angle β_T= 46.3-46.9^0 at all $\bar{\delta}_{bl}$=0.6-2.3%. A loading factor ψ_{T0}=0.859-0.878 is bigger when the blades are thicker.

The impeller #5 has β_{bl2}=32^0. Its angle β_T= 34.8-35.3^0 at all $\bar{\delta}_{bl}$=0.7-2.8%. A loading factor ψ_{T0}=0.848-0.856 is bigger when the blades are thicker.

The impeller #6 has β_{bl2}=32^0. It differs from the impeller #5 by smaller $\bar{b}_2$ only. Its angle β_T=32.2-32.4^0 at all $\bar{\delta}_{bl}$=0.7-2.8 %. A loading factor ψ_{T0}= 0.861-0.863 is constant practically too.

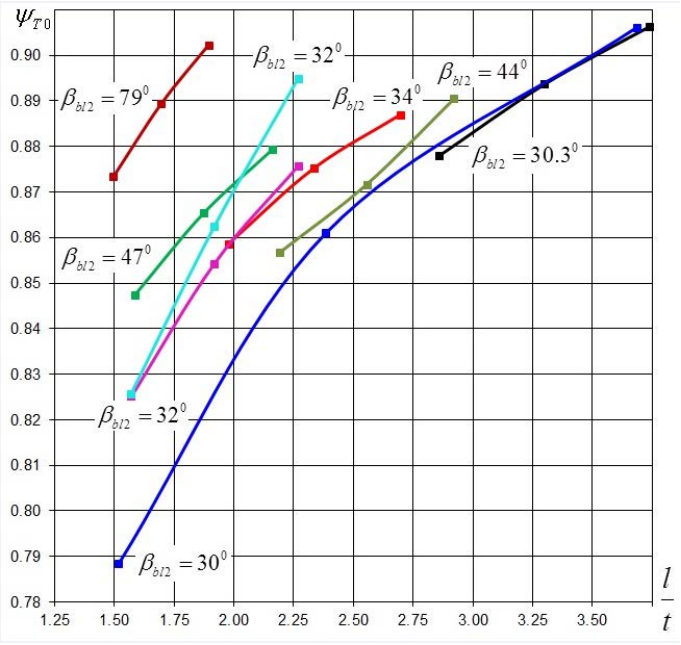

Fig. 11 Loading factor at zero flow coefficient for eight impellers with three number of blades each

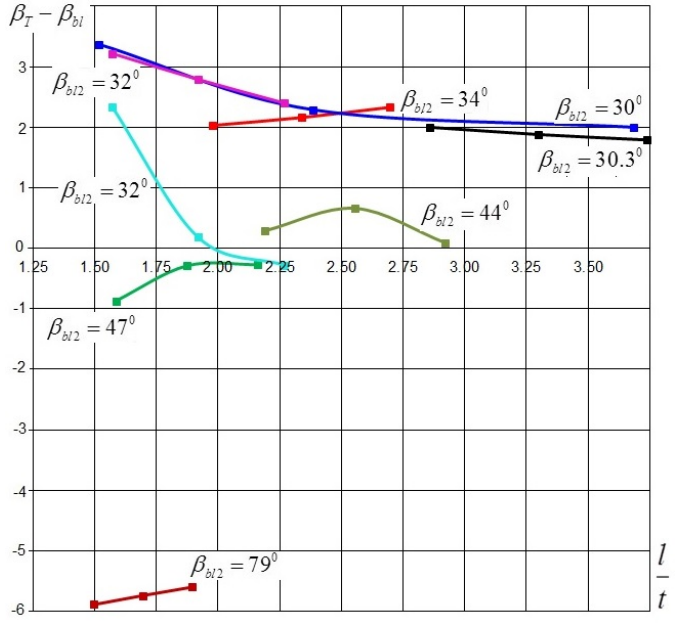

Fig. 12 Difference $\beta_T-\beta_{bl2}$ for eight impellers with three number of blades each

The impeller #7 has β_{bl2}=79^0. Its angle β_T=73.2-74.5^0 at all $\bar{\delta}_{bl}$=0.64-2.8 %. A loading factor ψ_{T0}= 0.876 – 0.91 is sufficiently bigger when the blades are thicker.

The impeller #8 has β_{bl2}=44^0. Its angle β_T=44.4-44.7^0 is constant practically and equal to blade exit angle at all $\bar{\delta}_{bl}$= 0.64-2.8%. A loading factor ψ_{T0}=0.870-0.882 is sufficiently bigger when the blades are thicker.

The influence of the blade thickness is rather small. Let us take into account that the range of $\bar{\delta}_{bl}$ exceeds the values that are applied usually.

VII. The Number of Blades, the Density of a Grid

Performances of eight initial impellers were calculated with bigger and smaller blade numbers. Traditionally, the number of blades is connected with a cascade solidity. In [8], two formulae are recommended:

$$\frac{l}{t} = z\frac{1-\bar{D}_1}{\pi\left(1+\bar{D}_1\right)\sin\left(\frac{\beta_{bl1}+\beta_{bl2}}{2}\right)} \quad (16)$$

$$\frac{l}{t} = z\frac{\lg\frac{D_2}{D_1}}{2.73\sin\left(\frac{\beta_{bl2}+\beta_{bl1}}{2}\right)}. \quad (17)$$

TABLE II
Performance Parameters for the Impellers with Different Number of Blades

№	Impeller name. Blade umber	β_{bl2}	z	$l/t(16a)$	$l/t(16b)$
1	028 z13	30.3	13	2.859	2.952
2	028 z 15	30.3	15	3.299	3.407
3	028 z17	30.3	17	3.739	3.861
4	038 z11	34	11	1.978	2.404
5	038 z 13	34	13	2.337	2.841
6	038-z15	34	15	2.697	3.279
7	048 z11	30	7	1.518	1.668
8	048 z13	30	11	2.385	2.622
9	048 z17	30	17	3.686	4.052
10	055 z11	47	11	1.585	2.059
11	055 z13	47	13	1.873	2.434
12	055 z15	47	15	2.162	2.808
13	060 z9	32	9	1.570	1.909
14	060 x 11	32	11	1.919	2.333
15	060 z13	32	13	2.268	2.757
16	064 z9	32	9	1.570	1.909
17	064 z11	32	11	1.919	2.333
18	064 z13	32	13	2.268	2.757
19	к 101-1 z15	79	15	1.495	1.986
20	к 101-1 z17	79	17	1.695	2.250
21	к 101-1 z19	79	19	1.894	2.515
22	к 101-4 z12	44	12	2.190	2.394
23	к 101-4 z14	44	14	2.556	2.793
24	к 101-4 z16	44	16	2.921	3.191

Table II contains results of calculations. Calculation results are presented in Figs. 11 and 12. Cascade solidity by (16) is the argument.

A loading factor at zero flow coefficient is obviously bigger if a cascade solidity is bigger. It is bigger also for impellers with the bigger blade exit angles. One more parameter influences as it is shown below. There are two exclusions for the impellers # 1 and 8 when this parameter changes little.

VIII. Ratio b_2/b_1 Influence

Eight centrifugal impellers have been calculated with a relative exit height of blades 20% more and 20% less than the original. There were compared three values of ratio influence for each impeller. The impellers # 5 and 6 differ only by this parameter. This series is of seven impellers only. The calculation results are presented in Table III.

TABLE III
Performance Parameters for the Impellers with Different Parameter b_2/b_1

№	Impeller name	b_2/b_1	β_T	β_{bl2}	$\frac{\beta_T-\beta_{bl2}}{\beta_{bl2}}$
1	028-b-0.0355	0.6027	32.81	30.3	0.083
2	028-0444-0589	0.7538	32.18	30.3	0.062
3	028-b-0.0533	0.9049	31.35	30.3	0.035
4	038-b-0.039	0.4716	37.42	34	0.101
5	038-0487-0827	0.5889	36.16	34	0.064
6	038-b-0.0584	0.7062	34.42	34	0.012
7	048-b-0.0288	0.3258	32.42	30	0.081
8	048-0576-0884	0.6516	32.29	30	0.076
9	048-b-0.0745	0.8428	33.75	30	0.125
10	055-b-0.044	0.4944	46.74	47	-0.006
11	055	0.618	46.43	47	-0.012
12	055-b-0.066	0.7416	44.49	47	-0.053
13	060-b-0.0484	0.4889	36.20	32	0.131
14	060	0.6111	34.79	32	0.087
15	060-b-0.0726	0.7333	33.81	32	0.057
16	064-b-0.056	0.5657	35.32	32	0.104
17	064	0.7071	32.18	32	0.006
18	064-b-0.084	0.8485	33.04	32	0.033
19	к 101-1-b-0.04	0.431	74.19	79	-0.061
20	к 101-1	0.5388	73.26	79	-0.073
21	к 101-1-b-0.06	0.6466	73.13	79	-0.074
22	к 101-4-b-0.017	0.5037	45.04	44	0.024
23	к 101-4	0.6296	44.66	44	0.015
24	к 101-4-b-0.068	0.7556	43.53	44	-0.011

Effect of b_2/b_1 on the coefficient ψ_{T0} is small and is not regular. The results are graphically represented in Fig. 13. Influence of b_2/b_1 on the angle β_T is sufficient. Graphics in Fig. 14 demonstrate it. When the ratio b_2/b_1 increases, the value of β_T decreases. The impeller #3 is the only exclusion. The influence of b_2/b_1 is less for impellers with bigger blade exit angle.

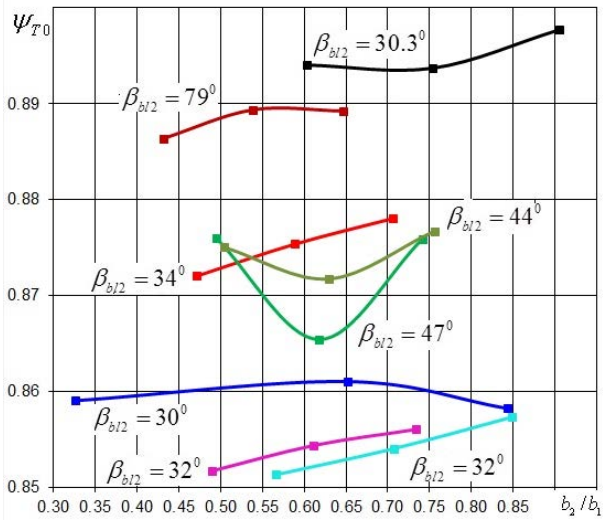

Fig. 13 Coefficient ψ_{T0} for seven Impellers with different ratio b_2/b_1

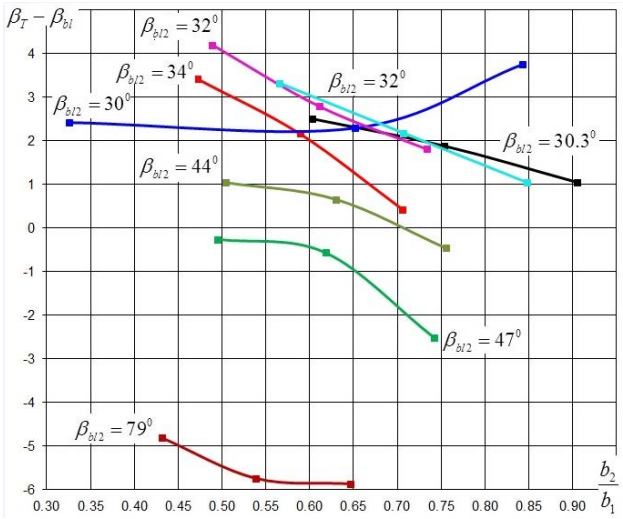

Fig. 14 Difference $\beta_T-\beta_{bl2}$ for seven impellers with different ratio b_2/b_1

IX. Blade Mean Line Configuration

Fig. 15 clarifies the difference of an arc mean line and a mean line optimized by load distribution.

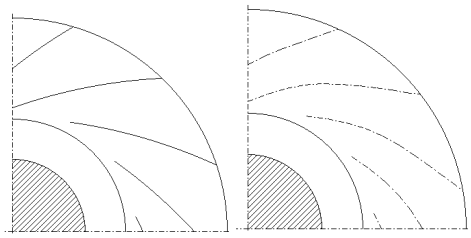

Fig. 15 Arc mean line of blades (a), and mean lines optimized by load distribution (b)

Blade profiling by the method of [3] is characterized by using the load shift to the trailing edge. Impeller performance shifts to left in comparison with arc blades. A loading factor is lower. Loading factor performances of the impellers #3-8 with profiled blades were calculated. Loading factor at zero flow coefficient for these impellers with arc and profiled blades are shown in Fig. 16. For arc blades, ψ_{T0} is bigger in all cases. As a rule, the difference is bigger for impellers with the bigger blade exit angles. Influence of the blade mean line configuration is presented in Fig. 17.

Angles of a performance inclination are bigger for arc blades. Bigger ψ_{T0} and β_T lead to sufficiently bigger loading factors at a design flow coefficient. This fact was proven experimentally, and the velocity diagrams demonstrated this effect too.

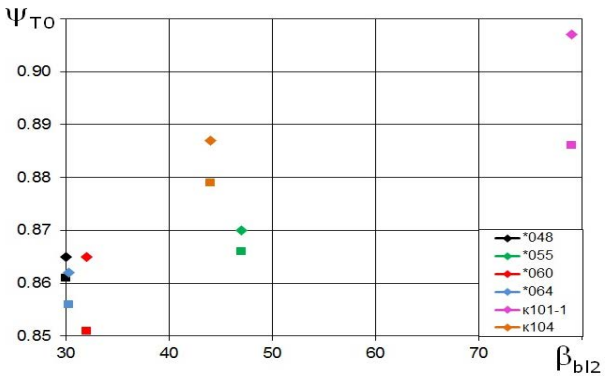

Fig. 16 Loading factor at zero flow coefficient for six impellers. Arc blades – rhombus. square – profiled blades

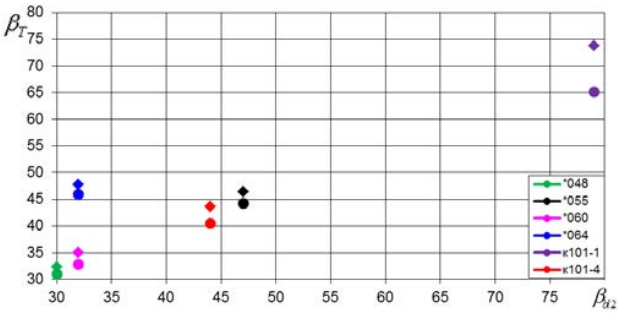

Fig. 17 Angle β_T for six impellers. Arc blades – rhombus. circle – profiled blades

X. Approximation of Calculation Results

To use in a mathematical model, the calculation results must be approximated by algebraic equations. At the moment, the authors offer simple algebraic equations that reflect the impact of the studied geometry parameters.

The equation for an angle of a performance inclination are:

- arc blades:

$$\psi_{T0} = 1 - \frac{100 - \beta_{bl2}}{y_1}\left(1 + y_2\beta_{bl2}\right)^3\left(1 - y_3\bar{\delta}_{bl}\right)\times \quad (18)$$
$$\times\left(1 - y_4 \cdot l/t\right)\left(1 - y_5 \cdot b_2/b_1\right)$$

- profiled blades:

$$\psi_{T0} = 1 - \frac{100 - \beta_{bl2}}{y_1}\left(1 + y_2\beta_{bl2}\right)^3\left(1 - y_3\bar{\delta}_{bl}\right)\times \quad (19)$$
$$\times\left(1 - y_4 \cdot l/t\right)\left(1 - y_5 \cdot b_2/b_1\right)\left(1 - 0.002\left(\beta_{bl}^0 - 20^0\right)\right)$$

The equations for the loading factor at zero flow coefficient are:

- arc blades:

$$\beta_T^0 = \beta_{bl}^0 + 0.17\left(45 - \beta_{bl}^0\right)\left(1 - 0.1\bar{\delta}_{bl} + \frac{0.02}{l/t} - \frac{0.02}{b_2/b_1}\right). \quad (20)$$

- profiled blades:

$$\beta_T^0 = \beta_{bl}^0 + \left[0.17\left(45 - \beta_{bl}^0\right)\left(1 - 0.1\bar{\delta}_{bl} + \frac{0.02}{l/t} - \frac{0.02}{b_2/b_1}\right)\right]\times \quad (21)$$
$$\times\left(1 - 0.28\left(\beta_{bl}^0 - 29^0\right)\right)$$

The precision of simulation is not very high. The general principle of a loading factor modeling more important. The next step – modeling of tested model stage performances the authors plan to start on principles above presented.

XI. Conclusion

Viscosity influence is necessary take into account first while modeling experimental performances. Other factors were not possible to study by the instrument that was used in the presented study. For instance, the type or configuration of a diffuser influences a loading factor. The final approximation equations will be more complicated and some sophisticated technologies could be applied. The authors aim inside this work was to discuss and get opinions of colleagues on the problem. It can be important for further progress.

References

[1] Seleznev. K. P. Galerkin. Y. B. Centrifugal compressors. // Leningrad. – 1982. – P. 271. (Russian).
[2] Soldatova. K. V. Analysis of gas flow in a gap «a shroud - casing» of a centrifugal compressor stage by numerical methods and design recommendations. Diss. Cand.Tech. sciences. // SPbTU. – SPb. – 2007. (Russian).
[3] Galerkin. Y. B. Tubrocompressors. LTD information and publishing center. - Moscow. – 2010. – P.650. (Russian).
[4] Galerkin. Y. B. Soldatova. K.V. Operational process modeling of industrial centrifugal compressors. Scientific bases. development stages. current state. Monograph. //St. Peterburg. - SPbTU. – 2011. (Russian).
[5] Galerkin Y. Rekstin A. Soldatova K. Gas dynamic design of the pipe line compressor with 90% efficiency. Model test approval. Conference "Compressors and their Systems". – London. – 2015.
[6] Galerkin Y. Karpov A. Development of method for centrifugal compressor impeller pressure characteristic modeling on results of model stages tests// Compressors & Pneumatics. – Moscow. - 2011. – No.6. – P.13-17. (Russian).
[7] Galerkin Y. Soldatova K. The application of the Universal Modeling Method to development of centrifugal compressor model stages. Conference "Compressors and their Systems". – 477-487. – London. – 2013. (Russian).
[8] Ris V. Centrifugal compressors. (text) / Ris V.// Leningrad. – 1981. (Russian).